

Characterizing graph symmetries through quantum Jensen-Shannon divergence

Luca Rossi,¹ Andrea Torsello,¹ Edwin R. Hancock,² and Richard C. Wilson²

¹*Dipartimento di Scienze Ambientali, Informatica e Statistica, Università Ca' Foscari Venezia, Via Torino 155, 30172 Venezia, Italy*

²*Department of Computer Science, University of York, York YO10 5DD, United Kingdom*

(Received 23 February 2013; published 10 September 2013)

In this paper we investigate the connection between quantum walks and graph symmetries. We begin by designing an experiment that allows us to analyze the behavior of the quantum walks on the graph without causing the wave function collapse. To achieve this, we base our analysis on the recently introduced quantum Jensen-Shannon divergence. In particular, we show that the quantum Jensen-Shannon divergence between the evolution of two quantum walks with suitably defined initial states is maximum when the graph presents symmetries. Hence, we assign to each pair of nodes of the graph a value of the divergence, and we average over all pairs of nodes to characterize the degree of symmetry possessed by a graph.

DOI: [10.1103/PhysRevE.88.032806](https://doi.org/10.1103/PhysRevE.88.032806)

PACS number(s): 89.75.Hc, 89.75.Kd, 89.75.Fb

I. INTRODUCTION

Recently, there has been increasing interest in using quantum walks as a primitive for designing novel quantum algorithms [1–4] on graph structures. Quantum walks on graphs represent the quantum mechanical analog of the classical random walk on a graph. Despite being similar in their definition, the dynamics of the two walks differ remarkably. This is mainly due to the fact that while the state vector of the classical random walk is real valued, in the quantum case the state vector is complex valued. This property allows different paths of the walk to interfere with each other in both constructive and destructive ways. In the classical case the evolution of the walk is governed by a double stochastic matrix, while in the quantum case the evolution is governed by a unitary matrix, thus rendering the walk reversible. This in turn implies that the quantum walk is nonergodic and, most importantly, it does not have a limiting distribution. Quantum walks have been extensively studied on a wide variety of graphs [5,6], such as the infinite line, cycles, regular lattices, star graphs, and complete graphs. Because of these properties, quantum walks have been shown to outperform their classical analog in a number of specific tasks, leading to polynomial and sometimes even exponential speedups over classical computation [7,8]. For example, Farhi and Gutmann [8] have shown that if we take two co-joined n -level binary trees that are connected at their leaves, a quantum walk commencing from the root of the first tree can hit the root of the second tree exponentially faster than a similarly defined classical random walk. The major contribution of Farhi and Gutmann's work [8] is to show that one may achieve an exponential speedup without relying on the quantum Fourier transform.

In the case of the co-joined trees graph described above, the presence of a symmetrical structure is of key importance to the speedup. Given a graph $G = (V, E)$, an automorphism is a permutation τ of the set of vertices V of the graph which preserves the adjacency relations, i.e., if $(u, v) \in E$, then $(\tau(u), \tau(v)) \in E$. The set of symmetries of G thus can be represented by its automorphism group $\text{Aut}(G)$. Figure 1 shows an example of a symmetric graph. Whenever the graph possess some kind of symmetry, the constructive interference between certain paths will lead to faster hitting

times. A number of recent works have further investigated the connection between the structural symmetries of the graph and the evolution of the quantum walk. For instance, Krovi and Brun [9] have proved that the phenomenon of infinite hitting times is generally a consequence of the symmetry of the graph and its automorphism group. Emms *et al.* [10] showed that there is a link between symmetries in the graph structure and a quasiquantum analog of the commute time. Specifically, the authors define a quasiquantum analog of the commute time associated with the continuous-time quantum walk and then explore the possibility of using it to embed the nodes of the graph into a low-dimensional vector space. Their work reveals that the symmetries of the graph correspond to degenerate directions in the quantum commute time embedding space. However, their analysis is not based on a principled observable and is, hence, semiclassical. Finally, Rossi *et al.* [11] have recently proposed a way to detect approximate axial symmetries in networks by measuring the interference patterns of continuous-time quantum walks. However, their analysis requires the observation of each of the possible states and thus is semiclassical, too.

The classical Jensen-Shannon divergence [12] is a measure of similarity between probability distributions that has its routes in information theory. Unlike the Kullback-Liebler divergence [13], it is both symmetric and directly linked to a metric (it is the square of a metric). Moreover, it can be used to define positive semidefinite kernels. As a result, the underlying metric space of probability distributions can be isometrically embedded in a real valued Hilbert-space. The quantum Jensen-Shannon divergence has recently been developed as a generalization of classical Jensen-Shannon divergence to quantum states by Majtey, Lamberti, and Prato [14–16]. For mixed quantum states they show that the quantum Jensen-Shannon divergence has good distinguishability properties. The quantum Jensen-Shannon divergence (QJSD) is defined in terms of the Von Neumann entropy and as such is not directly a quantum-mechanical observable, i.e., there is no operator whose expected value is the QJSD. However, it can be computed from density matrices whose entries are indeed observables.

In this work, we intend to investigate further the connection between quantum walks and graph symmetries, and, in

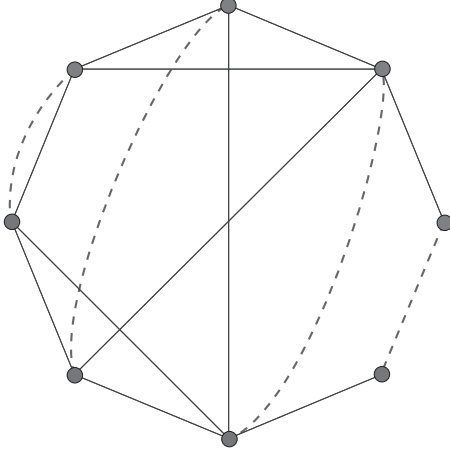


FIG. 1. An example of a graph displaying a symmetrical structure, where we highlighted the pairs of symmetrical vertices. Note that by permuting the pairs of linked nodes the adjacency relations are preserved.

particular, we study the quantum Jensen-Shannon divergence [15,16] between the evolution of two quantum walks on a graph with suitably defined initial states. Note, however, that while this analysis is fully based on observable properties and is not, thus, semiclassical like the one by Emms *et al.*, it is not meant to provide an algorithm exhibiting quantum speedup with respect to classical counterparts but rather to highlight how quantum walks can be used to provide information about the symmetric structure of a network.

The paper is organized as follows: Section II provides a brief introduction to continuous-time quantum walks, while Sec. III reviews the concepts of von Neumann entropy and quantum Jensen-Shannon divergence. In Sec. IV we introduce the link between graph symmetries and quantum walks and then propose a method to quantify the presence of symmetries in a graph based on the quantum Jensen-Shannon divergence. Section V illustrates the experimental results, while the conclusions are presented in Sec. VI.

II. CONTINUOUS-TIME QUANTUM WALKS

The continuous-time quantum walk [8] is a natural quantum analog of the classical random walk. Classical random walks model a diffusion process on a graph and have proven to be a useful tool in the analysis of its structure. Let $G = (V, E)$ be an undirected graph, where V is a set of n vertices and $E = (V \times V)$ is a set of edges. Diffusion on the graph is modeled as a Markovian process defined over V , with transitions restricted to adjacent vertices. More formally, we define the general state for the walk at time t as a probability distribution over V , i.e., a vector, $\mathbf{p}_t \in \mathbb{R}^n$, whose u th entry gives the probability that the walk is at vertex u at time t . Recall that the adjacency matrix of the graph G is the symmetric matrix with elements

$$A_{uv} = \begin{cases} 1 & \text{if } (u, v) \in E \\ 0 & \text{otherwise} \end{cases} \quad (1)$$

and let D be the diagonal matrix with elements $d_u = \sum_{v=1}^n A(u, v)$, where d_u is the degree of the node u . The *continuous-time random walk* on G then will evolve according

to the equation

$$\mathbf{p}_t = e^{-Lt} \mathbf{p}_0, \quad (2)$$

where $L = D - A$ is the graph Laplacian, a combinatorial analog of the Laplace-Beltrami operator [17].

The *continuous-time quantum walk*, i.e., the quantum counterpart of the continuous-time random walk, is similarly defined as a dynamical process over the vertices of the graph. By contrast to the classical case where the state vector is constrained to lie in a probability space, here the state of the system is defined through a vector of complex amplitudes over V whose squared norm sums to unity over the nodes of the graph, with no restriction on their sign or complex phase. These phase differences allow interference effects to take place. Moreover, in the quantum case the evolution of the state vector of the walker is governed by a complex valued unitary matrix, whereas the dynamics of the classical random walk is governed by a stochastic matrix. Hence, the evolution of the quantum walk is reversible, implying that quantum walks are nonergodic and do not possess a limiting distribution. As a result, the behavior of classical and quantum walks differs significantly, and quantum walks possess a number of interesting properties not exhibited by classical random walks.

More formally, using the Dirac notation, we denote the basis state corresponding to the walk being at vertex $u \in V$ as $|u\rangle$. A general state of the walk is a complex linear combination of the basis states, such that the state of the walk at time t is defined as

$$|\psi_t\rangle = \sum_{u \in V} \alpha_u(t) |u\rangle, \quad (3)$$

where the amplitude $\alpha_u(t) \in \mathbb{C}$ and $|\psi_t\rangle \in \mathbb{C}^{|V|}$ are both complex.

At each instant in time the probability of the walker being at a particular vertex of the graph is given by the square of the norm of the amplitude of the relative state. Let X^t be a random variable giving the location of the walker at time t . The probability of the walker being at the vertex u at time t then is given by

$$\Pr(X^t = u) = \alpha_u(t) \alpha_u^*(t), \quad (4)$$

where $\alpha_u^*(t)$ is the complex conjugate of $\alpha_u(t)$. Moreover, $\sum_{u \in V} \alpha_u(t) \alpha_u^*(t) = 1$ and $\alpha_u(t) \alpha_u^*(t) \in [0, 1]$ for all $u \in V$, $t \in \mathbb{R}^+$.

The evolution of the walk is then given by the Schrödinger equation, where we take the time-independent Hamiltonian of the system to be the graph Laplacian, yielding

$$\frac{\partial}{\partial t} |\psi_t\rangle = -iL |\psi_t\rangle. \quad (5)$$

Given an initial state $|\psi_0\rangle$, we can solve Eq. (5) to determine the state vector at time t ,

$$|\psi_t\rangle = e^{-iLt} |\psi_0\rangle. \quad (6)$$

Finally, we can compute the spectral decomposition of the graph Laplacian $L = \Phi \Lambda \Phi^\top$, where Φ is the $n \times n$ matrix $\Phi = (\phi_1 | \phi_2 | \dots | \phi_j | \dots | \phi_n)$ with the ordered eigenvectors ϕ_j s of L as columns and $\Lambda = \text{diag}(\lambda_1, \lambda_2, \dots, \lambda_j, \dots, \lambda_n)$ is the $n \times n$ diagonal matrix with the ordered eigenvalues λ_j of

L as elements, such that $0 = \lambda_1 \leq \lambda_2 \leq \dots \leq \lambda_n$. Using the spectral decomposition of the graph Laplacian and the fact that $\exp[-iLt] = \Phi \exp[-i\Lambda t] \Phi^\top$, we then can write

$$|\psi_t\rangle = \Phi e^{-i\Lambda t} \Phi^\top |\psi_0\rangle. \quad (7)$$

The observation process for a quantum system is defined in terms of projections onto orthogonal subspaces associated with operators on the quantum state space called *observables*. Let O be an observable of the system, with spectral decomposition

$$O = \sum_i a_i P_i, \quad (8)$$

where the a_i are the (distinct) eigenvalues of O and the P_i the orthogonal projectors onto the corresponding eigenspaces. An observation of a quantum state $|\psi\rangle$ is one of the eigenvalues a_i of O , which is observed with probability

$$P(a_i) = \langle \psi | P_i | \psi \rangle, \quad (9)$$

leaving the system in the state

$$|\bar{\psi}\rangle = \frac{P_i |\psi\rangle}{\|P_i |\psi\rangle\|}, \quad (10)$$

where $\| |\psi\rangle \| = \sqrt{\langle \psi | \psi \rangle}$ is the norm of the vector $|\psi\rangle$.

The *density operator* (or *density matrix*) is introduced in quantum mechanics to describe a system whose state is an ensemble of pure quantum states $|\psi_i\rangle$, each with probability p_i . The density operator of such a system is defined as

$$\rho = \sum_i p_i |\psi_i\rangle \langle \psi_i|. \quad (11)$$

Density operators are positive unit-trace matrices directly linked with the observables of the (mixed) quantum system. The expectation value of the measurement can be calculated from the density matrix ρ ,

$$\langle O \rangle = \text{tr}(\rho O), \quad (12)$$

where tr is the trace operator. Similarly, the observation probability of a_i can be expressed in terms of the density matrix ρ as

$$P(a_i) = \text{tr}(\rho P_i). \quad (13)$$

Finally, after the measurement, the corresponding density operator will be

$$\rho' = \sum_i P_i \rho P_i. \quad (14)$$

III. QUANTUM JENSEN-SHANNON DIVERGENCE

In this paper we intend to investigate how the presence of symmetries in the graph structure can alter the behavior of the quantum walker. To this end, for each walk we would like to study how the probability distribution over the state space varies with time. Unfortunately, when a measurement is made the wave function collapses and, with a probability equal to the squared norm of its amplitude, only one of the possible basis states is observed. In other words, if the state $|u\rangle$ is observed, after the measurement the new state of the quantum walk will be $|\psi\rangle = |u\rangle$. This implies that all

further information previously contained in the state is lost and further measurements will not yield any additional information about the premeasurement state. Hence, we need to design an experiment that will allow us to analyze the behavior of the quantum walk without causing the wave function collapse. In this section we will review the QJSD [14–16], a recently introduced distinguishability measure between quantum states. In Sec. IV we will use the QJSD to investigate the relation between graph symmetries and quantum walks.

The *von Neumann entropy* [18] H_N of a mixture is defined in terms of the trace and logarithm of the density operator ρ ,

$$H_N = -\text{tr}(\rho \log \rho) = -\sum_i \xi_i \ln \xi_i, \quad (15)$$

where ξ_1, \dots, ξ_n are the eigenvalues of ρ . If $\langle \psi_i | \rho | \psi_i \rangle = 1$, i.e., the quantum system is a pure state $|\psi_i\rangle$ with probability $p_i = 1$, then the von Neumann entropy $H_N(\rho) = -\text{tr}(\rho \log \rho)$ is zero. On other hand, for a mixed state described by the density operator σ we have a nonzero von Neumann entropy associated with it.

With the von Neumann entropy to hand, the quantum Jensen-Shannon divergence between two density operators ρ and σ is defined as

$$D_{JS}(\rho, \sigma) = H_N\left(\frac{\rho + \sigma}{2}\right) - \frac{1}{2}H_N(\rho) - \frac{1}{2}H_N(\sigma). \quad (16)$$

This quantity is always well defined, symmetric, and positive definite.

It can also be shown that $D_{JS}(\rho, \sigma)$ is bounded, i.e., $0 \leq D_{JS}(\rho, \sigma) \leq 1$. Let $\rho = \sum_i p_i \rho_i$ be a mixture of quantum states ρ_i , with $p_i \in \mathbb{R}^+$ such that $\sum_i p_i = 1$, and then one can prove that

$$H_N\left(\sum_i p_i \rho_i\right) \leq H_S(p_i) + \sum_i p_i H_N(\rho_i), \quad (17)$$

where H_S indicates the Shannon entropy and the equality is attained if and only if the states ρ_i have support on orthogonal subspaces. By setting $p_1 = p_2 = 0.5$, we see that

$$D_{JS}(\rho, \sigma) = H_N\left(\frac{\rho + \sigma}{2}\right) - \frac{1}{2}H_N(\rho) - \frac{1}{2}H_N(\sigma) \leq 1. \quad (18)$$

Hence, D_{JS} is always less than or equal to 1, and the equality is attained only if ρ and σ have support on orthogonal subspaces.

Our interest in the quantum Jensen-Shannon divergence lies in the fact that it verifies several interesting properties which are required for a good distinguishability measure between quantum states [15,16]. The problem of discriminating between two quantum states $|\phi\rangle$ and $|\psi\rangle$ of a given physical system is of central importance in quantum computation and quantum information, and it is based on the definition of a suitable distance measure. Recall that a function

$$d = \mathbb{X} \times \mathbb{X} \longrightarrow \mathbb{R} \quad (19)$$

defined over a set \mathbb{X} is a distance if, for every $x, y \in \mathbb{X}$,

$$d(x, y) \geq 0 \quad \text{with} \quad d(x, y) = 0 \iff x = y \quad (20)$$

and it is symmetric, i.e.,

$$d(x, y) = d(y, x). \quad (21)$$

Moreover, d is said to be a metric for \mathbb{X} if it satisfies the triangle inequality

$$d(x, y) + d(y, z) \geq d(x, z) \quad (22)$$

for every $x, y, z \in \mathbb{X}$.

In his seminal paper, Wootters [19] investigates the problem of distinguishability and defines the concept of statistical distance between pure quantum states. Here the distance between two different preparations $|\phi\rangle$ and $|\psi\rangle$ of the same physical system is computed by counting the number of distinguishable states between $|\phi\rangle$ and $|\psi\rangle$. The main result of Wootters's work is to show that this distance is equal to the angle in Hilbert space between $|\phi\rangle$ and $|\psi\rangle$. As a consequence, Wootters's distance is defined as

$$d_W(|\phi\rangle, |\psi\rangle) = \arccos(|\langle\phi|\psi\rangle|), \quad (23)$$

where $|\langle\phi|\psi\rangle|$ denotes the modulus of the inner product for ϕ and ψ . It can be proved that this distance satisfies the triangle inequality and is thus a metric.

Wootters's work is fundamentally based on the extension of a distance over the space of probability distributions to the Hilbert space of pure quantum states. Similarly, attempts to define a distance measure between pure and mixed quantum states are typically based on the generalization of divergence or distance measures commonly used in the space of probability distributions. This is the case of the relative entropy [20], which is a generalization of information theoretic Kullback-Leibler divergence. However, the relative entropy is neither a distance, as it is not symmetric, nor does it not satisfy the triangle inequality, and, most importantly, it is unbounded.

The square root of the QJSD, on the other hand, is bounded, it is a distance, and, as proved by Lamberti *et al.* [16], it satisfies the triangle inequality. In particular, the authors give a formal proof for the case of pure states, while for the case of mixed states they support their claim with numerical evidence. Note that alternative metrics have been proposed in the literature, such as the Bures distance [21], which is defined as

$$B(\rho, \sigma) = \sqrt{2[1 - \text{tr}((\rho^{1/2}\sigma\rho^{1/2})^{1/2})]^{1/2}}. \quad (24)$$

The Bures distance and the QJSD require the same number of observations, since they both need the full density matrices to be computed. However, the QJSD turns out to be faster to compute than the Bures distance. In fact, the latter involves taking the square root of matrices, usually computed through matrix diagonalization which scales as $O(n^3)$, where n is the number of vertices in the graph. On the other hand, to compute the QJSD only the eigenvalues of ρ , σ , and $\frac{\rho+\sigma}{2}$ are needed, which can be computed in $O(n^2)$. In the next section we propose to use the QJSD to measure the distance between suitably prepared quantum states to highlight the presence of symmetries in the structure of a graph.

IV. MEASURING SYMMETRIES

Given a pair of nodes $u \in V$ and $v \in V$ in an undirected graph $G = (V, E)$, we define two independent quantum walks with starting states

$$|\psi_0^-\rangle = \frac{|u\rangle - |v\rangle}{\sqrt{2}} \quad |\psi_0^+\rangle = \frac{|u\rangle + |v\rangle}{\sqrt{2}}, \quad (25)$$

where, and to recap our earlier definition, the basis state corresponding to the walk being at vertex $u \in V$ is denoted as $|u\rangle$. Intuitively, by setting the initial amplitude on the two nodes to be respectively in antiphase and in phase, we allow the walk to highlight the presence of destructive and constructive interference patterns on the graph. We then let the two quantum walks evolve under Eq. (6) until a time T and we define the average density operators ρ_T and σ_T over this time as

$$\rho_T = \frac{1}{T} \int_0^T |\psi_t^-\rangle \langle \psi_t^-| dt \quad \sigma_T = \frac{1}{T} \int_0^T |\psi_t^+\rangle \langle \psi_t^+| dt. \quad (26)$$

In other words, our system has equal probability of being in any of the pure states $|\psi_t^-\rangle$ ($|\psi_t^+\rangle$ respectively) defined by the quantum walk evolution.

Given this setting, we are now able to compute the quantum Jensen-Shannon divergence $D_{JS}(\rho_T, \sigma_T)$ between the two walks using Eq. (16). Due to the interference effect, we expect the mixed states for the two walks to have maximum divergence when the two initial nodes are symmetrically located in the graph. This is a consequence of the way in which we have initialized the two walks. Specifically, we aim to use the destructive and constructive interference effect by setting the initial node amplitudes to be respectively in antiphase and in phase. On the other hand, when the two nodes are not symmetrically located, then we expect the two resulting mixed states to be similar, thus yielding a low value of $D_{JS}(\rho_T, \sigma_T)$. In the following theorem we prove that when u and v are symmetrically placed, then ρ_T and σ_T have support on orthogonal subspaces, which implies $D_{JS}(\rho_T, \sigma_T) = 1$.

Theorem 1. Let ρ_T and σ_T be defined as in Eq. (26). If u, v are symmetrically placed and $|\psi_0^-\rangle$ and $|\psi_0^+\rangle$ are defined as in Eq. (25), then $D_{JS}(\rho_T, \sigma_T) = 1$.

Proof. We start by noting that if ρ_T and σ_T have support on orthogonal subspaces then

$$(\rho_T)^\dagger \sigma_T = \frac{1}{T^2} \int_0^T \rho_{t_1} dt_1 \int_0^T \sigma_{t_2} dt_2 = \mathbf{0}, \quad (27)$$

where $\mathbf{0}$ is the matrix of all zeros, $\rho_t = |\psi_t^-\rangle \langle \psi_t^-|$ and $\sigma_t = |\psi_t^+\rangle \langle \psi_t^+|$. Note that if $\rho_{t_1}^\dagger \sigma_{t_2} = \mathbf{0}$ for every t_1 and t_2 , then $(\rho_T)^\dagger \sigma_T = \mathbf{0}$. We hence can go on to show that if u and v are symmetric, then $\langle \psi_{t_1}^- | \psi_{t_2}^+ \rangle = 0$ for every t_1 and t_2 . Let $U^t = e^{-iLt}$. If $t_1 = t_2 = t$, then

$$\langle \psi_0^- | (U^t)^\dagger U^t | \psi_0^+ \rangle = 0, \quad (28)$$

since by definition $(U^t)^\dagger U^t$ is the identity matrix (since U is unitary) and the initial states are orthogonal by construction.

On the other hand, if $t_1 \neq t_2$, we need to prove that when u and v are symmetrical, then $|\psi_{t_1}^-\rangle$ and $|\psi_{t_2}^+\rangle$ are still orthogonal. In other words,

$$\langle \psi_0^- | U^{\Delta t} | \psi_0^+ \rangle = 0, \quad (29)$$

where $\Delta t = t_2 - t_1$. Recall that $\psi_0^- = 1/\sqrt{2}(|u\rangle - |v\rangle)$ and $\psi_0^+ = 1/\sqrt{2}(|u\rangle + |v\rangle)$. Then, if we denote by U_{ij}^t the ij -th element of U^t , we have that

$$\langle \psi_0^- | U^{\Delta t} | \psi_0^+ \rangle = U_{uu}^{\Delta t} - U_{vv}^{\Delta t} + U_{uv}^{\Delta t} - U_{vu}^{\Delta t}, \quad (30)$$

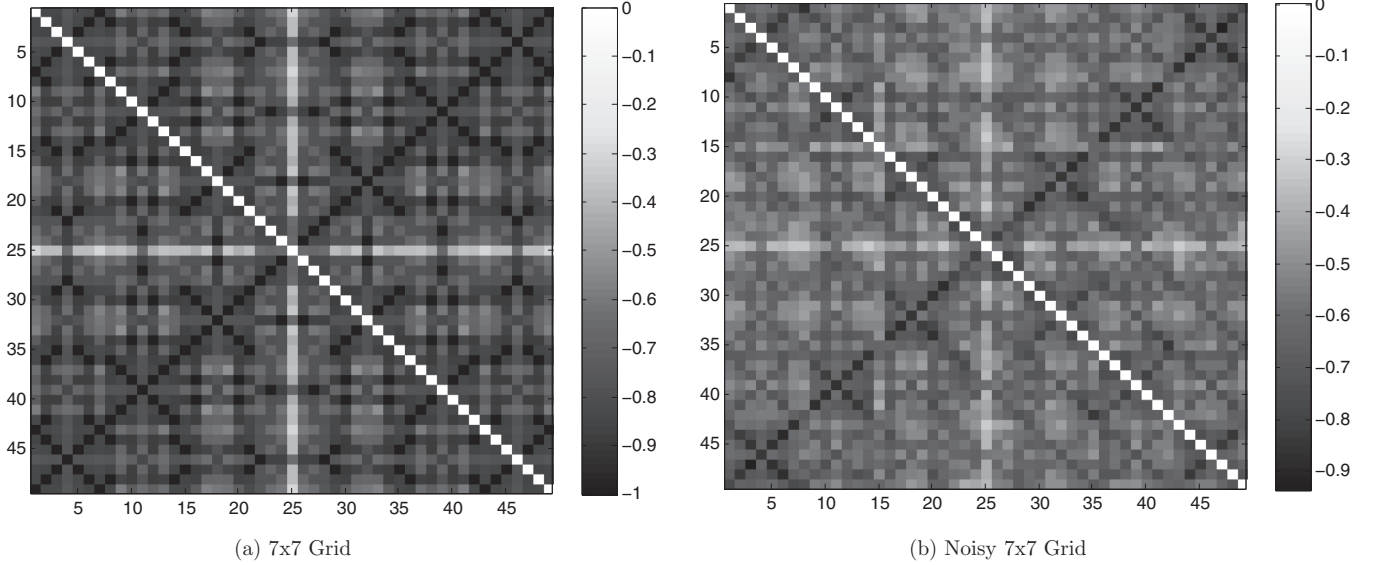


FIG. 2. The QJSD between pairs of walks initialized according to Eq. (25). Here the color indicates the value of the QJSD between two walks and the axes are indexed by the nodes, where the 49 nodes of the grid are numbered from 1 to 49 from left to right and from top to bottom. Note that the QJSD of the two walks is maximum (equal to 1) when the two walks are initialized on symmetrically placed nodes. If the symmetry is broken by deleting one edge (b), the QJSD remains considerably higher on approximately symmetrically placed nodes.

which further reduces to

$$\langle \psi_0^- | U^{\Delta t} | \psi_0^+ \rangle = U_{uu}^{\Delta t} - U_{vv}^{\Delta t} \quad (31)$$

since the matrix U^t is symmetric.

To conclude the proof, we prove that when u and v are symmetrical we have $U_{uu}^t = U_{vv}^t$. Recall that $U^t = e^{-iLt}$, where L is the graph Laplacian. If u and v belong to a symmetry orbit [a group of vertices where v_1 and v_2 belong to the same orbit if there is an automorphism $\tau \in \text{Aut}(G)$ such that $\tau(v_1) = v_2$], then there exists an automorphism of the graph with a corresponding permutation matrix \mathcal{P} such that

$$L = \mathcal{P}^\top L \mathcal{P} \quad (32)$$

and

$$\mathcal{P}|u\rangle = |v\rangle. \quad (33)$$

In other words, the graph Laplacian is invariant to symmetries. As we will show later, the same holds for the unitary operator of the quantum walk. In fact, given the spectral decomposition of the graph Laplacian $L = \Phi \Lambda \Phi^\top$, we can see that the following equality holds:

$$\Phi \Lambda \Phi^\top = \mathcal{P}^\top (\Phi \Lambda \Phi^\top) \mathcal{P} \quad (34)$$

and thus

$$\Phi = \mathcal{P}^\top \Phi. \quad (35)$$

Let us now write the unitary operator in terms of the Laplacian eigendecomposition, which yields

$$e^{-iLt} = \Phi e^{-i\Lambda t} \Phi^\top. \quad (36)$$

From Eqs. (35) and (36) it follows that

$$\Phi e^{-i\Lambda t} \Phi^\top = \mathcal{P}^\top \Phi e^{-i\Lambda t} \Phi^\top \mathcal{P}. \quad (37)$$

This in turn implies that if u and v are symmetrically placed, then $U_{uu}^t = U_{vv}^t$, which concludes the proof. ■

We should stress, however, that the converse of Theorem 1 does not hold. Note, in fact, that if we were able to prove the converse, then we could give a polynomial-time solution to the graph isomorphism problem.

The proof of Theorem 1 basically relies on the fact that whenever two nodes u and v are symmetrical, then $U_{uu}^t = U_{vv}^t$ for each time t , where U_{xx}^t is the wave kernel signature of x at time t . However, our analysis relies only on computing the divergence between two density operators, while directly observing the wave kernel signature would cause a collapse of the wave function. Note also that a similar analysis can be done by comparing the heat kernel signature [22] $\mathbf{h}(x) = (H_{xx}^{t_1}, H_{xx}^{t_2}, \dots, H_{xx}^{t_k})$ of u and v , where we denote by H_{xx}^t the solution of the heat equation at point x at time t . On a manifold, it can be shown that if $H_{uu}^t = H_{vv}^t$ for each t , then the two points have the same global geometry, which means they either are the same point or symmetrically placed, with respect to the intrinsic geometry. Note, however, that this only holds for points on a manifold.

Figure 2 shows the value of $D_{\text{JS}}(\rho_T, \sigma_T)$ for all the possible pairs of nodes with initial nonzero amplitude on a 7×7 grid with reflecting boundary conditions. In the remainder of the paper we will refer to this matrix as the QJSD matrix. As expected, the QJSD matrix clearly reveals the presence of several perfect symmetries, i.e., pair of nodes for which $D_{\text{JS}}(\rho_T, \sigma_T) = 1$. Note that if we randomly delete an edge the symmetries are very likely to be broken, as we observe in Fig. 2(b). Although we do not observe any perfect symmetry, the value of $D_{\text{JS}}(\rho_T, \sigma_T)$ remains higher on some pairs which were previously identified as being symmetrical, suggesting a connection between approximate symmetries and high values of the quantum Jensen-Shannon divergence.

To further support this claim, in Fig. 3 we show the value of the QJSD for a star graph with four nodes and a noisy version of it, where the noise is represented by an additional edge joining

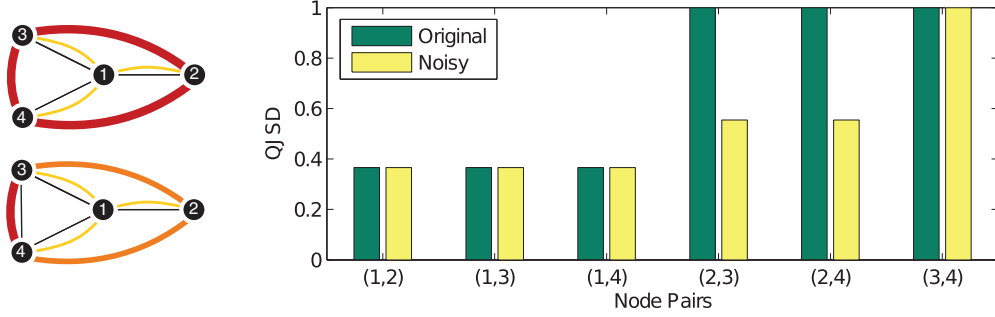


FIG. 3. (Color online) A star graph with four nodes and a modified version where two leaves are connected by an extra edge representing structural noise. The bar graph shows that although the symmetry between nodes 2,3 and 2,4 is broken with the addition of an extra edge, the QJSD is still sensibly higher for those pairs of nodes, suggesting the presence of an approximate symmetry.

nodes 3 and 4. Clearly, in the original star graph the three leaves are all symmetric with respect to the root node. However, if we alter the structure of the graph by adding an edge between 3 and 4, this results in breaking the symmetries between 2 and 3 and between 2 and 4 and, as a consequence, the QJSD between these nodes decreases. Interestingly, however, the QJSD for these pairs remains higher than the QJSD between 1 and 2, which is exactly what we would expect given the original symmetry.

A. Efficient computation of the QJSD

In this subsection we show how to compute the solution to Eq. (26) analytically. Let $P_\lambda = \sum_{k=1}^{\mu(\lambda)} \phi_{\lambda,k} \phi_{\lambda,k}^\top$ be the projection operator on the subspace spanned by the $\mu(\lambda)$ eigenvectors $\phi_{\lambda,k}$ associated with the eigenvalue λ of the graph Laplacian. The evolution operator of the quantum walk can be then expressed in terms of this set of projectors, i.e.,

$$U^t = \sum_{\lambda} e^{-i\lambda t} P_{\lambda}. \quad (38)$$

Recall that $|\psi_t\rangle = U^t |\psi_0\rangle$. According to Eq. (38), we can rewrite the density operator ρ_t associated with the pure state $|\psi_t\rangle$ as

$$\rho_t = U^t \rho_0 (U^t)^\dagger = \sum_{\lambda_1 \in \Lambda} \sum_{\lambda_2 \in \Lambda} e^{-i(\lambda_1 - \lambda_2)t} P_{\lambda_1} \rho_0 P_{\lambda_2}^\top. \quad (39)$$

As a consequence, we can reformulate Eq. (26) as

$$\rho_T = \frac{1}{T} \int_0^T \rho_t dt = \sum_{\lambda_1 \in \Lambda} \sum_{\lambda_2 \in \Lambda} P_{\lambda_1} \rho_0 P_{\lambda_2}^\top \frac{1}{T} \int_0^T e^{-i(\lambda_1 - \lambda_2)t} dt. \quad (40)$$

Solving the integral in Eq. (40) finally yields

$$\rho_T = \sum_{\lambda_1 \in \Lambda} \sum_{\lambda_2 \in \Lambda} P_{\lambda_1} \rho_0 P_{\lambda_2}^\top \frac{i(1 - e^{iT(\lambda_2 - \lambda_1)})}{T(\lambda_2 - \lambda_1)}. \quad (41)$$

Note that if we let $T \rightarrow \infty$, then the integral in Eq. (40) reduces to the Dirac delta function $\delta(\lambda_1 - \lambda_2)$. Hence, Eq. (40)

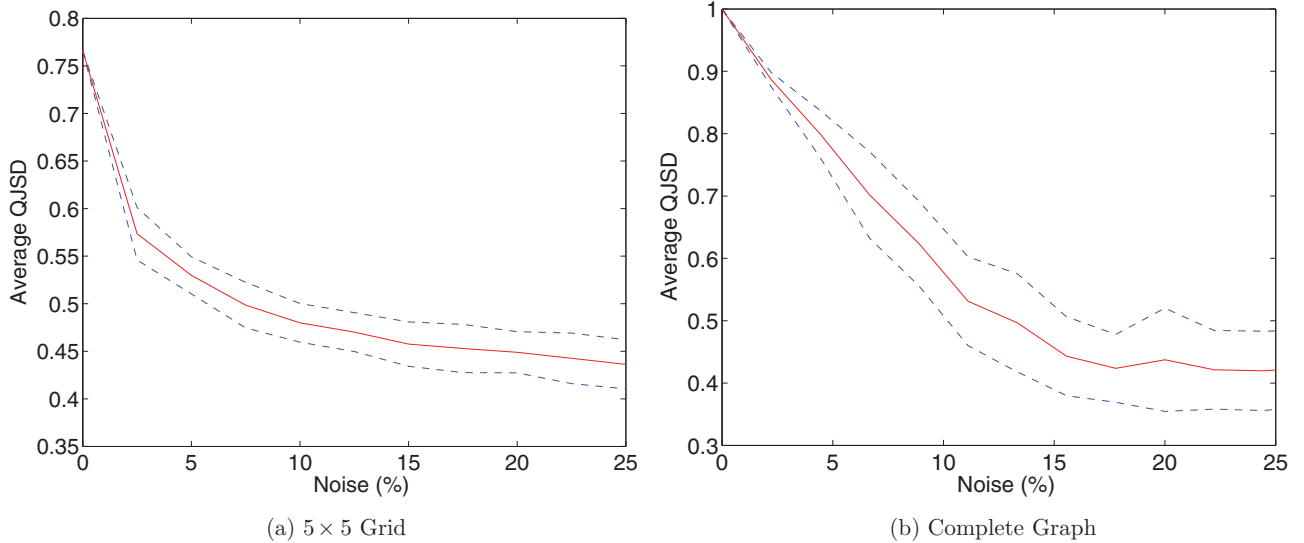


FIG. 4. (Color online) The average QJSD as a function of the structural (edge) noise for a 5×5 grid and a complete graph. Adding by randomly deleting (inserting) edges has the effect of breaking the symmetries of the original graphs and as a consequence the average QJSD decreases. Here the solid line indicates the mean, while the dashed lines indicate the standard deviation.

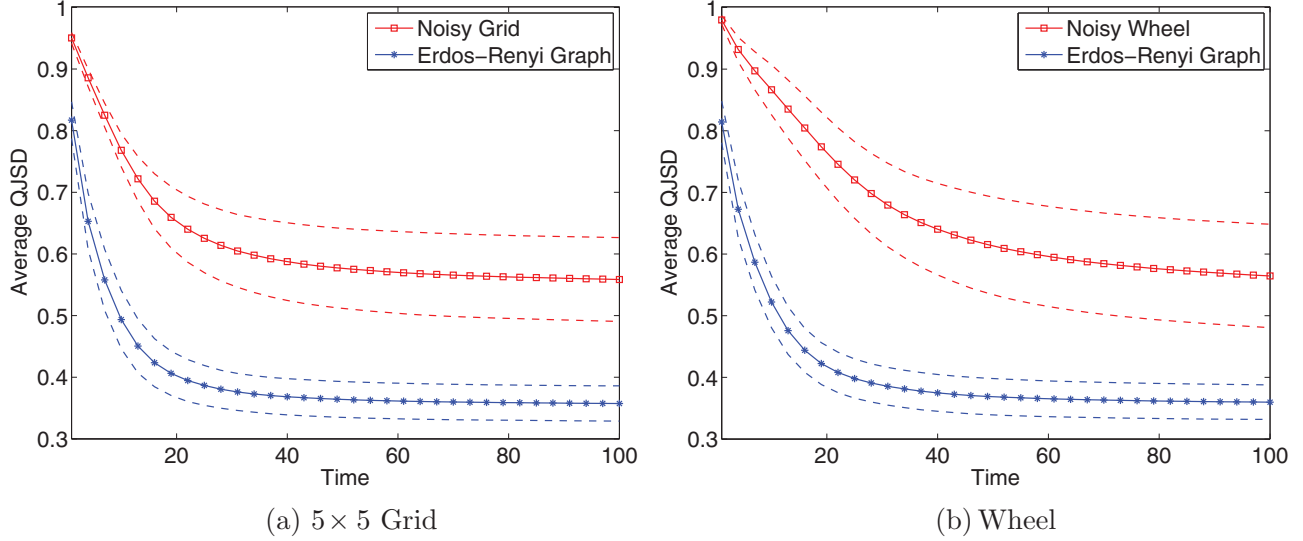


FIG. 5. (Color online) The average of the QJSD matrix clearly distinguishes between a random graph and a symmetrical graph where artificial noise is added. Here the solid line indicates the mean, while the dashed lines indicate the standard deviation.

simplifies to

$$\rho_{\infty} = \sum_{\lambda \in \tilde{\Lambda}} P_{\lambda} \rho_0 P_{\lambda}^{\top}, \quad (42)$$

where $\tilde{\Lambda}$ is the set of distinct eigenvalues of the graph Laplacian, i.e., the eigenvalues λ with multiplicity $\mu(\lambda) = 1$. A consequence of Eq. (42) is that the infinite-time limit of the average density matrix commutes with the graph Laplacian L , in fact

$$\begin{aligned} L\rho_{\infty} &= \left(\sum_{\lambda \in \tilde{\Lambda}} \lambda P_{\lambda} P_{\lambda}^{\top} \right) \left(\sum_{\lambda \in \tilde{\Lambda}} P_{\lambda} \rho_0 P_{\lambda}^{\top} \right) = \sum_{\lambda \in \tilde{\Lambda}} P_{\lambda} \lambda \rho_0 P_{\lambda}^{\top} \\ &= \left(\sum_{\lambda \in \tilde{\Lambda}} P_{\lambda} \rho_0 P_{\lambda}^{\top} \right) \left(\sum_{\lambda \in \tilde{\Lambda}} \lambda P_{\lambda} P_{\lambda}^{\top} \right) = \rho_{\infty} L. \end{aligned} \quad (43)$$

Hence, given the spectral decomposition of the graph Laplacian $L = \Phi \Lambda \Phi^{\top}$, the density matrix, expressed in the eigenvector basis given by Φ , assumes a block-diagonal form, where each block corresponds to an eigenspace of L corresponding to a single eigenvalue. Thus, if L has all eigenvalues distinct, then ρ_{∞} expressed in the unique eigenbasis of L will be diagonal and its diagonal entries will directly correspond to its eigenvalues. More generally, to compute the eigenvalues of ρ_{∞} , we need to solve independently for the eigenvalues of each diagonal block, resulting in a complexity $O(\sum_{\lambda \in \tilde{\Lambda}} \mu(\lambda)^2)$, where $\mu(\lambda)$ is the multiplicity of the eigenvalue λ .

V. EXPERIMENTAL RESULTS

In this section we intend to use the QJSD matrix to measure the degree of symmetry possessed by a graph. The basic requirements of this measure should be (a) that its value increases (decreases) as the number of approximate symmetries of the graph increases (decreases), (b) that it is permutation invariant, and (c) possibly easy to compute. Here we choose to use the average of the QJSD matrix as a simple yet effective means of characterising the degree of

symmetry possessed by a graph. Although it is known that as a statistic the average lacks robustness, since it is significantly affected by outliers, our experiments show that it provides a fast and permutation invariant way of measuring the degree of symmetry of a graph. More precisely, we investigate how the average QJSD over the pair of nodes varies for increasing time intervals. To this end, we numerically simulate the evolution of the two quantum walks with starting states as defined in Eq. (25) using the software package MATLAB.

In our first experiment, we take a 5×5 grid with reflecting boundary conditions and a complete graph of size 10 and we iteratively add structural noise by deleting an increasing number of edges at each step. The procedure is repeated 100 times, and for each level of noise we compute the mean over the 100 trials of the average QJSD on the noisy graphs, where for each pair of nodes the QJSD is computed as in Eq. (42). Figure 4 shows the result, where the structural noise affects from 0% to 25% of the graph edges. Here the solid line indicates the mean, while the dashed line indicates the standard deviation over the 100 repeated trials. Note that as the noise increases, the graphs become less and less symmetric, and at the same time the average QJSD rapidly decreases. This seems to fit with our hypothesis that the average QJSD can be used as a simple indicator of the degree of symmetry of a graph.

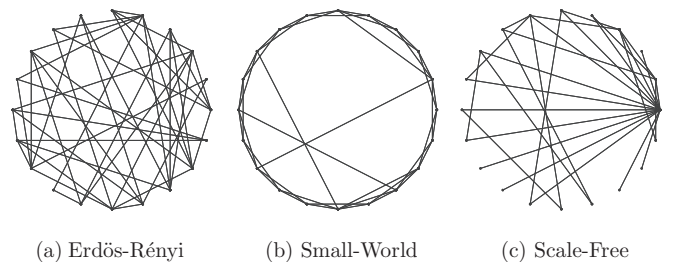
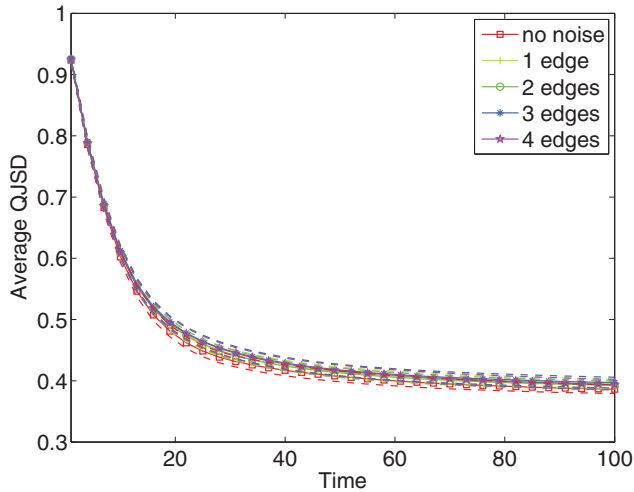
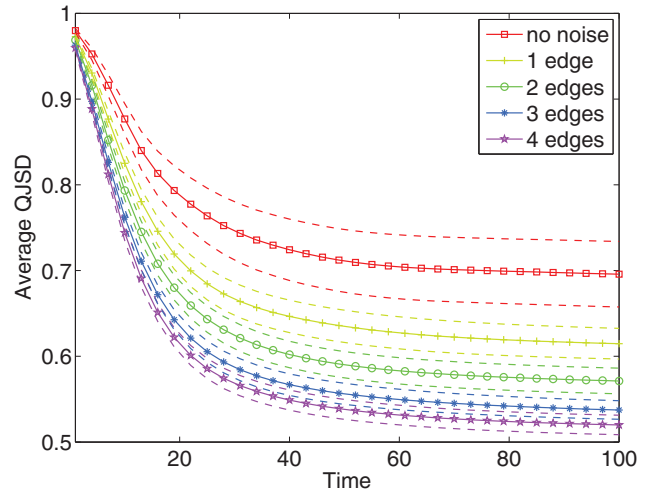


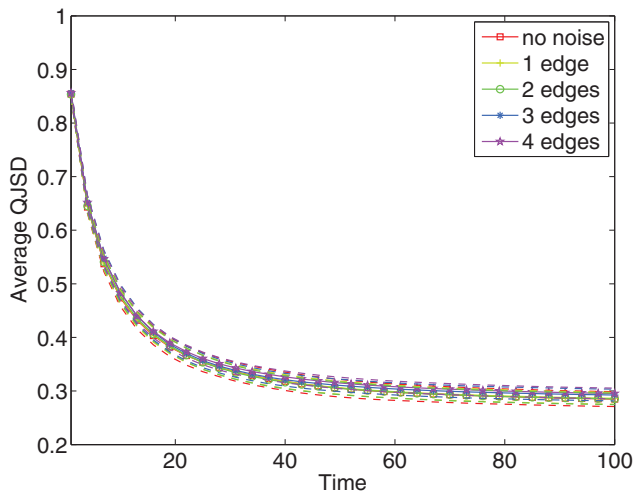
FIG. 6. Examples of graphs generated by the Erdős-Rényi, Watts-Strogatz, and Barabási-Albert models, respectively.



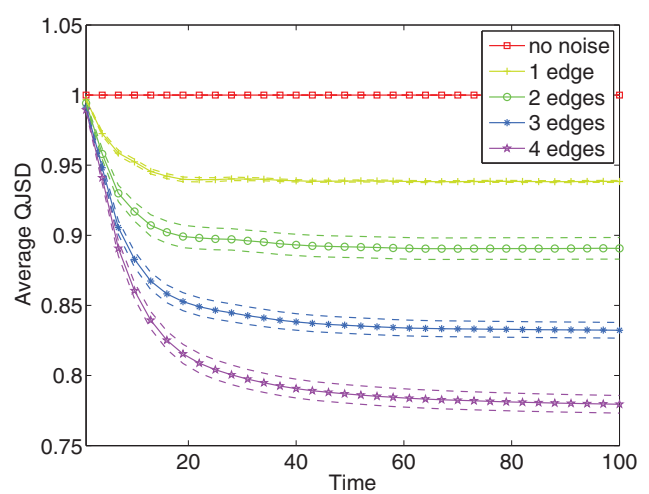
(a) Erdős-Rényi



(b) Small-World



(c) Scale-Free



(d) Strongly Regular

FIG. 7. (Color online) The effects of noise on the mean of the QJSD matrix on different type of networks for time intervals of increasing length. Note that here the solid line indicates the mean, while the dashed lines indicates the standard error.

As a second experiment, we take the same 5×5 grid and we randomly create noisy versions of it by adding or deleting up to three edges at random locations. We then compare the average QJSD (over all pairs of nodes) on these graphs with that of a set of Erdős-Rényi random graphs. Figure 5 shows the average of the QJSD matrix for time intervals of increasing length. Again, the solid line indicates the mean, while the dashed line indicates the standard deviation over 100 trials. As we can see, we are able to completely discriminate between the noisy versions of the 5×5 grid and the Erdős-Rényi graphs. This seems to confirm our intuition that the average QJSD matrix is able to capture the presence of (approximate) symmetrical patterns in a graph. We repeat the same experiment, but this time we perturb the 32-cycle graph where we have added a central axis of symmetry which connects an opposite pair of vertices. Again, the perturbed versions of the modified 32-cycle graph have a higher average QJSD when compared to Erdős-Rényi random graphs.

As a third experiment, we select three different random network models, namely the Watts-Strogatz [23], the Barabási-Albert [24], and the Erdős-Rényi [25] models. The Erdős-Rényi random graphs are generated by connecting pairs of nodes in the graphs with a uniform probability p . The Watts-Strogatz model produces small-world networks with a high clustering coefficient and a short average path length. Finally, the preferential attachment algorithm of Barabási and Albert generates scale-free networks. In this type of random graph the degree distribution of the vertices follows the power-law distribution, which is a property observed in many real-world networks. In Fig. 6, we show some examples of Erdős-Rényi, small-world, and scale-free random graphs. We add to these three network models a set of strongly regular graphs. A regular graph with v vertices and degree k is said to be strongly regular if there are two integers ε and θ such that every two adjacent vertices have ε common neighbors and every two nonadjacent vertices have θ common neighbors. We choose strongly regular

graphs because they are known to be highly symmetric and this should be reflected in the value of the QJSD.

We can see from Fig. 7 that we are able to discriminate these three types of random graphs by observing the average QJSD. In particular, due to their nature, the small-world graphs seem to have more symmetries than the two alternative models. In fact, the small-world network is constructed by randomly linking the nodes of a regular ring lattice, thus yielding an interpolation between an Erdős-Rényi graph and a regular graph. Note also that the average QJSD is reduced by adding or deleting random edges, since this amounts to hiding the symmetrical patterns under increasing levels of noise. Although reduced, the average QJSD for the small-world networks remains considerably higher than that of the Erdős-Rényi and scale-free graphs, where the addition of random noise does not seem to alter the average QJSD. As expected, the high number of symmetries possessed by strongly regular graphs is reflected in the higher value of the average QJSD, which remains clearly distinct from the three random networks even in the presence of Erdős-Rényi noise. Note also that if the graph structure of the strongly regular graph is not perturbed, the QJSD between each pair of nodes is maximum, i.e., each pair of nodes is in a symmetrical relation. Finally, although the behavior of the scale-free and Erdős-Rényi graphs is somewhat similar under noise, it is still possible to distinguish between them. In other words, the average QJSD of a scale-free graph is generally lower than that of an Erdős-Rényi graph.

VI. CONCLUSIONS

Much recent research in the quantum walks domain has shown the existence of a link between the interesting properties shown by quantum walks on graphs and the presence of symmetrical motifs in the graphs structure. This particular structure, in fact, can lead to remarkable interference effects, both constructive and destructive. In this paper we have proposed a way to measure the presence of symmetries in a graph using the quantum Jensen-Shannon divergence. This in turn has allowed us to design an experiment to analyze the behavior of the quantum walk without causing the wave function collapse. We showed how to define two mixed states based on two different quantum walks on the graph, and we used the resulting density operators to measure the distance between the two quantum states. In particular, we proved that when the graph possess a symmetry, the QJSD between the two quantum states is maximum. Our experiments show that a simple measure such as the average of the QJSD matrix is able to capture the structural difference between a symmetrical graph and an Erdős-Rényi random graph, even in the presence of moderate Erdős-Rényi noise, as well as to distinguish between different random network models.

ACKNOWLEDGMENT

E.H. was supported by a Royal Society Wolfson Research Merit Award.

-
- [1] J. Kempe, *Contemp. Phys.* **44**, 307 (2003).
 - [2] A. Ambainis, *Int. J. Quantum. Inform.* **1**, 507 (2003).
 - [3] A.M. Childs, *Phys. Rev. Lett.* **102**, 180501 (2009).
 - [4] M. Santha, *Lect. Notes Comput. Sc.* **4978**, 31 (2008).
 - [5] O. Mülken and A. Blumen, *Phys. Rep.* **502**, 37 (2011).
 - [6] V. Kendon, *Math. Struct. Comput. Sci.* **17**, 1169 (2007).
 - [7] N. Shenvi, J. Kempe, and K. Birgitta Whaley, *Phys. Rev. A* **67**, 052307 (2003).
 - [8] E. Farhi and S. Gutmann, *Phys. Rev. A* **58**, 915 (1998).
 - [9] H. Krovi and T. A. Brun, *Phys. Rev. A* **74**, 042334 (2006).
 - [10] D. Emms, R. Wilson, and E. R. Hancock, *Quantum Inf. Comput.* **9**, 231 (2009).
 - [11] L. Rossi, A. Torsello, and E. R. Hancock, *Lect. Notes Comput. Sc.* **7626**, 144 (2012).
 - [12] J. Lin, *IEEE Trans. Inf. Theory* **37**, 145 (1991).
 - [13] S. Kullback, *Information Theory and Statistics* (Dover, London, 1997).
 - [14] A. P. Majtey, P. W. Lamberti, M. Martin, and A. Plastino, *Eur. Phys. J. D* **32**, 413 (2005).
 - [15] A. P. Majtey, P. W. Lamberti, and D. P. Prato, *Phys. Rev. A* **72**, 052310 (2005).
 - [16] P. W. Lamberti, A. P. Majtey, A. Borras, M. Casas, and A. Plastino, *Phys. Rev. A* **77**, 052311 (2008).
 - [17] J. Jost, *Riemannian Geometry and Geometric Analysis* (Springer, Berlin, 2011).
 - [18] M. Nielsen and I. Chuang, *Quantum Computation and Quantum Information* (Cambridge University Press, Cambridge, 2010).
 - [19] W. K. Wootters, *Phys. Rev. D* **23**, 357 (1981).
 - [20] G. Lindblad, *Commun. Math. Phys.* **33**, 305 (1973).
 - [21] D. Bures, *Transact. Am. Math. Soc.* **135**, 199 (1969).
 - [22] J. Sun, M. Ovsjanikov, and L. Guibas, *In Computer Graphics Forum*, Vol. 28 (Blackwell Publishing Ltd, Oxford, 2009), pp. 1383–1392.
 - [23] D. J. Watts and S. H. Strogatz, *Nature* **393**, 440 (1998).
 - [24] A. Barabási and R. Albert, *Science* **286**, 509 (1999).
 - [25] P. Erdős and A. Rényi, *Publ. Math. Debrecen* **6**, 290 (1959).